

Then, for $\bar{z} = g^2 \bar{w}$, the composite pdf $f_{\bar{z}}(\bar{z})$ from $f_Q(q)$ and $f_{\bar{w}}(\bar{w})$ can be obtained as

$$\begin{aligned} f_{\bar{z}}(\bar{z}) &= \int_{-\infty}^{\infty} \frac{1}{|q|} f_Q(q) f_{\bar{w}}\left(\frac{\bar{z}}{q}\right) dq \\ &= \frac{10}{\ln 10 \sqrt{2\pi} \sigma_x \Gamma^2(N)} \int_0^{\infty} \frac{1}{q^2} e^{-\frac{(5 \log_{10} q)^2}{2\sigma_x^2}} \\ &\quad \times \left(\frac{\bar{z}}{q}\right)^{N-1} K_0\left(2\sqrt{\frac{\bar{z}}{q}}\right) dq \end{aligned} \quad (25)$$

where $dq/dx = q(\ln 10/5)$. With a change of variables $y^2 = (5 \log_{10} q)^2 / 2\sigma_x^2$, (25) can be rewritten as

$$\begin{aligned} f_{\bar{z}}(\bar{z}) &= \frac{2}{\sqrt{\pi} \Gamma^2(N)} \int_{-\infty}^{\infty} e^{-y^2} \left(\frac{1}{10^{\sqrt{2}\sigma_x y/5}}\right) \\ &\quad \times \left(\frac{\bar{z}}{10^{\sqrt{2}\sigma_x y/5}}\right)^{N-1} K_0\left(2\sqrt{\frac{\bar{z}}{10^{\sqrt{2}\sigma_x y/5}}}\right) dy. \end{aligned} \quad (26)$$

ACKNOWLEDGMENT

The authors would like to thank the editor and the reviewers for their constructive suggestions.

REFERENCES

- [1] S. M. Alamouti, "A simple transmit diversity technique for wireless communications," *IEEE J. Sel. Areas Commun.*, vol. 16, no. 8, pp. 1451–1458, Oct. 1998.
- [2] V. Tarokh, N. Seshadri, and A. R. Calderbank, "Space-time codes for high data rates wireless communications: Performance criterion and code construction," *IEEE Trans. Inf. Theory*, vol. 44, no. 2, pp. 744–765, Mar. 1998.
- [3] R. Prasad and A. Kegel, "Effects of Rician faded and lognormal shadowed signals on spectrum efficiency in microcellular radio," *IEEE Trans. Veh. Technol.*, vol. 42, no. 3, pp. 274–281, Aug. 1993.
- [4] M. K. Simon and M.-S. Alouini, *Digital Communication Over Fading Channels*. New York: Wiley, 2002.
- [5] C. Tellambura, A. J. Mueller, and V. K. Bhargava, "Analysis of M-ary phase-shift keying with diversity reception for land mobile satellite channels," *IEEE Trans. Veh. Technol.*, vol. 46, no. 4, pp. 910–922, Nov. 1997.
- [6] A. Conti, M. Z. Win, M. Chiani, and J. H. Winters, "Bit error outage for diversity reception in shadowing environment," *IEEE Commun. Lett.*, vol. 7, no. 1, pp. 15–17, Jan. 2003.
- [7] G. Zang and G. Li, "Performance analysis of orthogonal space-time block codes over shadowed Rician fading channels," in *Proc. IEEE ITW*, Punta del Este, Uruguay, Oct. 2006, pp. 453–457.
- [8] A. Nezampour and R. Schober, "Asymptotic analysis of space-time codes in generalized fading channels," *IEEE Commun. Lett.*, vol. 13, no. 8, pp. 561–563, Aug. 2009.
- [9] M. Z. A. Khan and B. S. Rajan, "Single-symbol maximum likelihood decodable linear STBCs," *IEEE Trans. Inf. Theory*, vol. 52, no. 5, pp. 2062–2091, May 2006.
- [10] H. Lee, J. G. Andrews, and E. J. Powers, "Information outage probability and diversity order of symmetric coordinate interleaved orthogonal designs," *IEEE Trans. Wireless Commun.*, vol. 7, no. 5, pp. 1501–1506, May 2008.
- [11] H. Lee, J. G. Andrews, R. W. Heath, Jr., and E. J. Powers, "The performance of space-time block codes from coordinate interleaved orthogonal designs over Nakagami- m fading channels," *IEEE Trans. Commun.*, vol. 57, no. 3, pp. 653–664, Mar. 2009.
- [12] M. Abramowitz and I. A. Stegun, *Handbook of Mathematical Functions*. New York: Dover, 1972.
- [13] G. L. Stüber, *Principles of Mobile Communication*, 2nd ed. Norwell, MA: Kluwer, 2001.
- [14] L.-L. Yang and W. Fang, "Performance of distributed-antenna DS-CDMA systems over composite lognormal shadowing and Nakagami- m -fading channels," *IEEE Trans. Veh. Technol.*, vol. 58, no. 6, pp. 2872–2883, Jul. 2009.
- [15] I. M. Kostic, "Analytical approach to performance analysis for channel subject to shadowing and fading," *Proc. Inst. Elect. Eng.—Commun.*, vol. 152, no. 6, pp. 821–827, Dec. 2005.
- [16] H. Shin and J. H. Lee, "Performance analysis of space-time block codes over keyhole Nakagami- m fading channels," *IEEE Trans. Veh. Technol.*, vol. 53, no. 2, pp. 351–362, Mar. 2004.

Low-Complexity Iterative Frequency Domain Decision Feedback Equalization

Chao Zhang, Zhaocheng Wang, *Senior Member, IEEE*,
Changyong Pan, *Member, IEEE*, Sheng Chen, *Fellow, IEEE*,
and Lajos Hanzo, *Fellow, IEEE*

Abstract—Single-carrier transmission with frequency-domain equalization (SC-FDE) offers a viable design alternative to the classic orthogonal frequency-division multiplexing (OFDM) technique. However, SC-FDE using a linear equalizer may suffer from serious performance deterioration for transmission over severely frequency-selective fading channels. An effective method of solving this problem is to introduce nonlinear decision feedback equalization (DFE) to SC-FDE. In this paper, a low-complexity iterative DFE operating in the frequency domain of single-carrier systems is proposed. Based on the minimum-mean-square-error (MMSE) criterion, a simplified parameter estimation method is introduced to calculate the coefficients of the feedforward and feedback filters, which significantly reduces the implementation complexity of the equalizer. Simulation results show that the performance of the proposed simplified design is similar to the traditional iterative block DFE under various multipath fading channels, but it imposes a much lower complexity than the latter.

Index Terms—Decision feedback equalizer (DFE), iterative block DFE (IBDFE), minimum mean square error (MMSE), single-carrier frequency-domain equalization.

I. INTRODUCTION

Single-carrier (SC) transmission [1], [2] and multicarrier orthogonal frequency-division multiplexing (OFDM) [3] are two main techniques that have been widely used in recent years for broadband high-rate wireless communication systems. Due to its ability to suppress intersymbol interference caused by multipath fading channels using a single-tap frequency-domain (FD) equalizer, OFDM has been

Manuscript received June 3, 2010; revised December 20, 2010; accepted January 16, 2011. Date of publication January 28, 2011; date of current version March 21, 2011. This work was supported by Tsinghua University Initiative Scientific Research Program 20091081280. The review of this paper was coordinated by Dr. C. Cozzo.

C. Zhang, Z. Wang, and C. Pan are with the State Key Laboratory on Microwave and Digital Communications, Tsinghua National Laboratory of Information Science and Technology, Department of Electronic Engineering, Tsinghua University, Beijing 100084, China (e-mail: z_c@tsinghua.edu.cn; zcwang@tsinghua.edu.cn; pcy@tsinghua.edu.cn).

S. Chen and L. Hanzo are with the School of Electronics and Computer Science, University of Southampton, SO17 1BJ Southampton, U.K. (e-mail: sqc@ecs.soton.ac.uk; lh@ecs.soton.ac.uk).

Color versions of one or more of the figures in this paper are available online at <http://ieeexplore.ieee.org>.

Digital Object Identifier 10.1109/TVT.2011.2109017

adopted in numerous wireless communication standards, such as wireless local area networks [4], digital video broadcasting [5], and the Third-Generation Partnership Project Long-Term Evolution (3GPP LTE) [6]. However, high peak-to-average-power ratio (PAPR) [3] and sensitivity to carrier offset and phase noise are some major problems associated with OFDM systems. SC transmission with FD equalization (SC-FDE) [1], [2] provides an attractive design alternative to OFDM for broadband wireless communications. It avoids using complex time-domain (TD) high-order equalizers in the case of channel dispersion spanned over many SC symbols by applying single-tap FDE after the discrete Fourier transformation (DFT). SC-FDE has a similar implementation complexity and performance to OFDM systems [7]. As an added benefit due to the low PAPR, SC techniques are more suitable for uplink applications, which require energy-efficient and low-cost power amplifiers in handsets. SC-FDE has also been selected as one of the alternative technical solutions in the IEEE 802.16 standard [8] and has been adopted for the uplink of the 3GPP LTE [6].

FD linear equalization (FD-LE) of SC systems is proposed based on the zero-forcing or minimum-mean-square-error (MMSE) criterion in [9]. However, FD-LE suffers from significant noise enhancement for transmission over deep frequency-selective fading channels, which may result in considerable performance degradation. An effective method of overcoming the problems associated with FD-LE is to use decision feedback equalizer (DFE). In [1] and [10], a hybrid equalization architecture known as the SC-FDE-DFE is proposed for SC systems, in which the FD-LE acts as feedforward equalizer, whereas a TD transversal filter is adopted for feedback equalization. A similar FD-DFE structure using TD noise prediction is given in [11]. However, a matrix inversion operation is required in the DFE structures of [1], [10], and [11], where the order of the matrix depends on the number of the taps in the TD feedback filter. This limits the length of the feedback equalizer, which has considerable influence on the achievable equalization performance. A soft-interference-cancellation-aided MMSE equalizer is proposed in [12] for the SC cyclic-prefix (CP)-based multiuser system, which is more general than the single-user system considered in this paper. The work in [13] analyzes the turbo FDE, where the channel decoder and an MMSE-based FD-LE iteratively exchange information, which is beyond the scope of this study.

In [14], an iterative block DFE (IBDFE) based on the MMSE criterion is studied, in which both the feedforward and feedback filters operate in the FD by using DFT and inverse DFT (IDFT) operations. The matrix inversion required in the hybrid equalizer structures of [1], [10], and [11] is thus eliminated. However, in each iteration of the feedback, the cross-correlation function between the detected symbols and the transmitted symbols has to be calculated. Furthermore, the estimation of the signal-to-noise ratio (SNR) is also needed. As a result, the system complexity of the IBDFE is increased. In this paper, a low-complexity iterative DFE operating in the FD and based on the MMSE criterion is proposed as a design alternative to the IBDFE benchmark. We introduce the variance of the decision errors at each iteration, which is related to the symbol error rate (SER) at each iteration. By adopting a predefined SER value and an approximate SNR value, the calculation of the filter coefficients is considerably simplified. In particular, the coefficients of the feedforward and feedback equalizers are only calculated once, and they do not need updating at each iteration. This is in contrast to the IBDFE, which requires recalculating the coefficients of the two filters at each iteration. As a result, our proposed scheme significantly reduces the computational complexity required, in comparison with the IBDFE. We demonstrate that our scheme achieves the same equalization performance as the IBDFE; furthermore, its bit error rate (BER) performance is not sensitive to the predefined SER and SNR estimates.

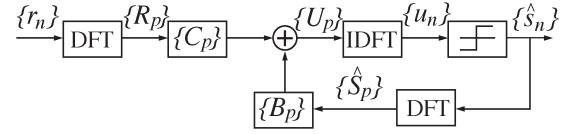


Fig. 1. System model of the IBDFE.

The rest of this paper is organized as follows: Section II introduces the system model and the IBDFE benchmark [14]. Section III first analyzes the parameter calculations of the DFE structure based on the MMSE criterion. Then, approximation to the parameter estimation is proposed, and the complexity reduction of our simplified design over the IBDFE is quantified. Our simulation results are presented in Section IV, whereas our conclusions are provided in Section V.

II. SYSTEM MODEL

Consider an SC block transmission system, where the serial binary data streams are mapped to the complex-valued symbol streams with symbol rate f_s according to the modulation mode. Then, the symbol streams are grouped into information data blocks having a length of M . We drop the block index and simply denote a data block as $\{d_m\}_{m=0}^{M-1}$. A known pseudorandom noise (PN) sequence having the length of N , i.e., $\{\varepsilon_n\}_{n=0}^{N-1}$, is inserted at the beginning of the transmission frame as the preamble. Each information data block is also concatenated with this PN sequence to form a transmission block having the length of $P = M + N$, which is expressed as

$$\begin{aligned} \mathbf{s} &= [s_0, s_1, \dots, s_{P-1}]^T \\ &= [d_0, d_1, \dots, d_{M-1}, \varepsilon_0, \varepsilon_1, \dots, \varepsilon_{N-1}]^T. \end{aligned} \quad (1)$$

Assume that the maximum multipath delay spread of the channel is shorter than N/f_s and that the transmission data block \mathbf{s} is filtered by the channel having the channel impulse response (CIR) \mathbf{h} to yield the received signal block $\mathbf{r} = [r_0, r_1, \dots, r_{P-1}]^T$. Since the known PN sequence in the previous block can be regarded as the CP of the current transmission block by viewing the previous PN sequence and the current block as a “virtual” block, \mathbf{r} can be treated as the circular convolution between the transmission data block and the CIR. Let $\mathbf{R} = [R_0, R_1, \dots, R_{P-1}]^T$, $\mathbf{S} = [S_0, S_1, \dots, S_{P-1}]^T$, and $\mathbf{H} = [H_0, H_1, \dots, H_{P-1}]^T$ be the P -point DFTs of \mathbf{r} , \mathbf{s} , and \mathbf{h} , respectively, and define $\mathbf{W} = [W_0, W_1, \dots, W_{P-1}]^T$ as the DFT of the channel's additive white Gaussian noise. Then, the FD received signal becomes

$$R_p = H_p S_p + W_p, \quad 0 \leq p \leq P-1. \quad (2)$$

The receiver structure of the IBDFE [14] is shown in Fig. 1, which consists of the feedforward equalizer and the feedback filter. Assuming that the equalizer iterates L times, the coefficients of the feedforward and feedback equalizers can be expressed as $\mathbf{C}^{(l)} = [C_0^{(l)}, C_1^{(l)}, \dots, C_{P-1}^{(l)}]^T$ and $\mathbf{B}^{(l)} = [B_0^{(l)}, B_1^{(l)}, \dots, B_{P-1}^{(l)}]^T$, respectively, where $l = 1, \dots, L$ is the iteration index. At the $(l-1)$ th iteration, the equalized signal $\mathbf{U}^{(l-1)} = [U_0^{(l-1)}, U_1^{(l-1)}, \dots, U_{P-1}^{(l-1)}]^T$ is converted from the FD to the TD by the IDFT to yield $\mathbf{u}^{(l-1)} = [u_0^{(l-1)}, u_1^{(l-1)}, \dots, u_{P-1}^{(l-1)}]^T$. After the decision, the detected symbol block $\hat{\mathbf{s}}^{(l-1)} = [\hat{s}_0^{(l-1)}, \hat{s}_1^{(l-1)}, \dots, \hat{s}_{P-1}^{(l-1)}]^T$ is generated, which is then converted back to the FD by the DFT to produce $\hat{\mathbf{S}}^{(l-1)} =$

$[\hat{S}_0^{(l-1)}, \hat{S}_1^{(l-1)}, \dots, \hat{S}_{P-1}^{(l-1)}]^T$. Then, the equalized signals represented in the FD and the TD at the l th iteration are given by

$$U_p^{(l)} = C_p^{(l)} R_p + B_p^{(l)} \hat{S}_p^{(l-1)}, \quad 0 \leq p \leq P-1 \quad (3)$$

$$u_n^{(l)} = \frac{1}{P} \sum_{p=0}^{P-1} U_p^{(l)} e^{j \frac{2\pi}{P} p n}, \quad 0 \leq n \leq P-1 \quad (4)$$

respectively. The respective coefficients of the feed-forward and feedback filters derived in [14] are given by

$$C_p^{(l)} = \frac{H_p^*}{\sigma_W^2 + \sigma_S^2 \left(1 - \frac{|\rho_{S, \hat{S}^{(l-1)}}|^2}{\sigma_S^2 \sigma_{\hat{S}^{(l-1)}}^2} \right) |H_p|^2} \quad (5)$$

$$B_p^{(l)} = -\frac{\rho_{S, \hat{S}^{(l-1)}}}{\sigma_{\hat{S}^{(l-1)}}^2} \left(H_p C_p^{(l)} - \frac{1}{P} \sum_{k=0}^{P-1} H_k C_k^{(l)} \right) \quad (6)$$

where H_p^* denotes the conjugate of H_p ; σ_W^2 and σ_S^2 are the FD powers of the noise and transmission data block, respectively; $\sigma_{\hat{S}^{(l-1)}}^2$ is the FD power of the detected symbols at the l th iteration; and $\rho_{S, \hat{S}^{(l-1)}}$ is the FD cross correlation between the transmitted data symbols and the previous detected symbols, which is defined by $\rho_{S, \hat{S}^{(l-1)}} = E[S_p (\hat{S}_p^{(l-1)})^*]$.

The noise power σ_W^2 in (5) has to be estimated. Furthermore, it is clear that, in each iteration, the cross-correlation function $\rho_{S, \hat{S}^{(l-1)}}$ and the signal power at the detection point $\sigma_{\hat{S}^{(l-1)}}^2$ have to be estimated to recalculate the two filters' coefficients. The parameters $\rho_{S, \hat{S}^{(l-1)}}$ and $\sigma_{\hat{S}^{(l-1)}}^2$ can be estimated at each iteration according to

$$\rho_{S, \hat{S}^{(l-1)}} = \frac{1}{P_S} \sum_{p \in P_S} \frac{R_p}{H_p} (\hat{S}_p^{(l-1)})^* \quad (7)$$

$$\sigma_{\hat{S}^{(l-1)}}^2 = \frac{1}{P_S} \sum_{p \in P_S} |\hat{S}_p^{(l-1)}|^2 \quad (8)$$

respectively, where P_S is the cardinality of the set of frequencies $S = \{p : 1 \leq p \leq P \text{ and } |H_p| > H_{TH}\}$, whereas H_{TH} is a given channel gain threshold.

The computational complexity of the IDFT and DFT signal processing associated with the IBDFFE can be shown to be $2(P/2 \log_2 P + P)L$ complex multiplications and $2LP \log_2 P + P(L-1)$ complex additions [15]. In addition

$$\begin{aligned} (6P_S + 7P + 4)(L-1) + 6P + 3M & \quad \text{multiplications} \\ (6P_S + 5P - 2)(L-1) + 5P + 3M - 4 & \quad \text{additions} \end{aligned} \quad (9)$$

are required by the IBDFFE to compute the two filters' parameters in L iterations, where the so-called M_2M_4 SNR estimator of [16] is used to estimate σ_W^2 with M data symbols.

III. PROPOSED DECISION FEEDBACK EQUALIZATION ARCHITECTURE

In this section, the proposed DFE based on the MMSE criterion is first presented, followed by our simplified design method for the associated parameter calculation.

A. Parameter Design

Let us express the FD feedback signal $\hat{\mathbf{S}}^{(l-1)}$ as

$$\hat{S}_p^{(l-1)} = S_p + \Xi_p^{(l-1)}, \quad 0 \leq p \leq P-1 \quad (10)$$

where $\Xi_p^{(l-1)}$ denotes the FD decision error between the transmitted symbol S_p and the detected symbol $\hat{S}_p^{(l-1)}$ in the $(l-1)$ th iteration, which has a variance $\sigma_{\Xi^{(l-1)}}^2$. Then, we have

$$U_p^{(l)} = C_p^{(l)} R_p + B_p^{(l)} (S_p + \Xi_p^{(l-1)}). \quad (11)$$

At the l th iteration, the mean square error (MSE) at the decision point is given by

$$\begin{aligned} \text{MSE}^{(l)} &= \frac{1}{P} \sum_{n=0}^{P-1} E[|u_n^{(l)} - s_n|^2] \\ &= \frac{1}{P^2} \sum_{p=0}^{P-1} E[|U_p^{(l)} - S_p|^2]. \end{aligned} \quad (12)$$

Substituting (11) into (12) leads to

$$\begin{aligned} \text{MSE}^{(l)}(\mathbf{C}^{(l)}, \mathbf{B}^{(l)}) &= \frac{1}{P^2} \sum_{p=0}^{P-1} E[|C_p^{(l)} R_p + B_p^{(l)} (S_p + \Xi_p^{(l-1)}) - S_p|^2] \\ &= \frac{1}{P^2} \sum_{p=0}^{P-1} \left\{ |C_p^{(l)} H_p + B_p^{(l)} - 1|^2 \sigma_S^2 + |C_p^{(l)}|^2 \sigma_W^2 + |B_p^{(l)}|^2 \sigma_{\Xi^{(l-1)}}^2 \right. \\ &\quad \left. + 2\Re[(C_p^{(l)} H_p + B_p^{(l)} - 1)(B_p^{(l)})^* \Gamma^{(l-1)}] \right\} \end{aligned} \quad (13)$$

where $\Re[\bullet]$ denotes the real part, and $\Gamma^{(l-1)} = E[S_p (\Xi_p^{(l-1)})^*]$.

The MMSE solution for $C_p^{(l)}$ and $B_p^{(l)}$ is obtained by minimizing the MSE, i.e., $\text{MSE}^{(l)}(\mathbf{C}^{(l)}, \mathbf{B}^{(l)})$ of (13), under the constraint of [14]

$$\sum_{p=0}^{P-1} B_p^{(l)} = 0. \quad (14)$$

Let us construct the Lagrangian associated with this constrained optimization

$$f(\mathbf{C}^{(l)}, \mathbf{B}^{(l)}, \lambda^{(l)}) = \text{MSE}^{(l)}(\mathbf{C}^{(l)}, \mathbf{B}^{(l)}) + \lambda^{(l)} \sum_{p=0}^{P-1} B_p^{(l)} \quad (15)$$

where $\lambda^{(l)}$ is the Lagrange multiplier. By setting the gradients of $f(\mathbf{C}^{(l)}, \mathbf{B}^{(l)}, \lambda^{(l)})$ with respect to $C_p^{(l)}$, $B_p^{(l)}$, and $\lambda^{(l)}$ to zero, respectively, we have

$$\begin{aligned} \frac{\partial f(\mathbf{C}^{(l)}, \mathbf{B}^{(l)}, \lambda^{(l)})}{\partial C_p^{(l)}} &= \frac{1}{P^2} [(C_p^{(l)} H_p - 1) H_p^* \sigma_S^2 \\ &\quad + H_p^* B_p^{(l)} (\sigma_S^2 + (\Gamma^{(l-1)})^*) + C_p^{(l)} \sigma_W^2] = 0 \end{aligned} \quad (16)$$

$$\begin{aligned} & \frac{\partial f(\mathbf{C}^{(l)}, \mathbf{B}^{(l)}, \lambda^{(l)})}{\partial B_p^{(l)}} \\ &= \frac{1}{P^2} [B_p^{(l)} (\sigma_S^2 + 2\Re[\Gamma^{(l-1)}] + \sigma_{\Xi}^2) \\ & \quad + (C_p^{(l)} H_p - 1) (\sigma_S^2 + \Gamma^{(l-1)})] + \lambda^{(l)} = 0 \end{aligned} \quad (17)$$

$$\begin{aligned} & \frac{\partial f(\mathbf{C}^{(l)}, \mathbf{B}^{(l)}, \lambda^{(l)})}{\partial \lambda^{(l)}} \\ &= \sum_{p=0}^{P-1} B_p^{(l)} = 0. \end{aligned} \quad (18)$$

From (17), the parameters $B_p^{(l)}$ can be expressed as

$$B_p^{(l)} = -\frac{(C_p^{(l)} H_p - 1) (\sigma_S^2 + \Gamma^{(l-1)}) + P^2 \lambda^{(l)}}{\sigma_S^2 + 2\Re[\Gamma^{(l-1)}] + \sigma_{\Xi}^2} \quad (19)$$

with $p = 0, 1, \dots, P-1$. When using (18), (19) can be rewritten as

$$B_p^{(l)} = -\frac{\sigma_S^2 + \Gamma^{(l-1)}}{\sigma_S^2 + 2\Re[\Gamma^{(l-1)}] + \sigma_{\Xi}^2} (C_p^{(l)} H_p - \gamma^{(l)}) \quad (20)$$

with $p = 0, 1, \dots, P-1$, and

$$\gamma^{(l)} = \frac{1}{P} \sum_{m=0}^{P-1} C_m^{(l)} H_m. \quad (21)$$

By substituting (20) into (16), the parameters $C_p^{(l)}$ can be expressed as

$$C_p^{(l)} = \frac{\left(\sigma_S^2 - \frac{|\sigma_S^2 + \Gamma^{(l-1)}|^2}{\sigma_S^2 + 2\Re[\Gamma^{(l-1)}] + \sigma_{\Xi}^2} \gamma^{(l)} \right) H_p^*}{\sigma_W^2 + \left(\sigma_S^2 - \frac{|\sigma_S^2 + \Gamma^{(l-1)}|^2}{\sigma_S^2 + 2\Re[\Gamma^{(l-1)}] + \sigma_{\Xi}^2} \right) |H_p|^2} \quad (22)$$

where $p = 0, 1, \dots, P-1$. By combining (21) and (22), we have

$$\gamma^{(l)} = \sigma_S^2 \Phi^{(l)} \left(1 + \frac{|\sigma_S^2 + \Gamma^{(l-1)}|^2}{\sigma_S^2 + 2\Re[\Gamma^{(l-1)}] + \sigma_{\Xi}^2} \Phi^{(l)} \right)^{-1} \quad (23)$$

where

$$\Phi^{(l)} = \frac{1}{P} \sum_{p=0}^{P-1} \frac{|H_p|^2}{\sigma_W^2 + \left(\sigma_S^2 - \frac{|\sigma_S^2 + \Gamma^{(l-1)}|^2}{\sigma_S^2 + 2\Re[\Gamma^{(l-1)}] + \sigma_{\Xi}^2} \right) |H_p|^2}. \quad (24)$$

Based on (20)–(24), we can see that the estimates of the parameters σ_W^2 , σ_{Ξ}^2 , and $\Gamma^{(l-1)}$ are required at each iteration, whereas σ_S^2 is a known value that is determined by the symbol constellation employed. Specifically, the FD power σ_S^2 of the transmitted symbols is related to the TD power $\sigma_s^2 = E[|s_n|^2]$ of the TD transmitted signal $\{s_n\}_{n=0}^{P-1}$ by

$$\sigma_S^2 = E \left[\sum_{n_1=0}^{P-1} s_{n_1} e^{-j\frac{2\pi}{P} n_1 p} \sum_{n_2=0}^{P-1} s_{n_2}^* e^{j\frac{2\pi}{P} n_2 p} \right] = P\sigma_s^2. \quad (25)$$

We now consider how to effectively estimate σ_{Ξ}^2 , $\Gamma^{(l-1)}$, and σ_W^2 or SNR.

B. Parameter Estimation

Estimation of σ_{Ξ}^2 : The power of the decision errors σ_{Ξ}^2 is determined by the modulation mode and the SER. For Gray-coded quadrature amplitude modulation (QAM), the estimation of σ_{Ξ}^2 can be determined as follows: At low SERs, we assume that the decision error will always corrupt the decision into one of the adjacent symbols, which implies that only one of the in-phase or quadrature components will be erroneous [17]. Accordingly, σ_{Ξ}^2 of different QAM schemes can be expressed as

$$\sigma_{\Xi}^2 = \beta \sigma_S^2 P_s^{(l-1)} \quad (26)$$

where $\beta = 2, 2/5$ and $2/21$ for 4QAM, 16QAM, and 64QAM, respectively, and $P_s^{(l-1)}$ denotes the SER at the $(l-1)$ th iteration. To simplify the computational requirements, we assume that the SER at each iteration remains approximately unchanged, and we further fix $P_s^{(l-1)}$ in (26) to a predefined SER value $P_{s,\text{pre}}$. Note that, to successfully apply decision feedback, the initial SER of the linear equalizer should be below a certain threshold. The value of $P_{s,\text{pre}}$ may be chosen according to this threshold.

Estimation of $\Gamma^{(l-1)}$: The estimation of $\Gamma^{(l-1)}$ is also related to the modulation mode and the SER. From the Cauchy inequality, it is clear that

$$\begin{aligned} |\Gamma^{(l-1)}|^2 &= \left| \frac{1}{P} \sum_{p=0}^{P-1} S_p (\Xi_p^{(l-1)})^* \right|^2 \\ &< \frac{1}{P^2} \left(\sum_{p=0}^{P-1} |S_p|^2 \right) \left(\sum_{p=0}^{P-1} |(\Xi_p^{(l-1)})^*|^2 \right) \\ &= \sigma_S^2 E \left[|\Xi_p^{(l-1)}|^2 \right]. \end{aligned} \quad (27)$$

Let $\{\xi_n^{(l-1)}\}_{n=0}^{P-1}$ represent the TD decision errors, where we have

$$\Xi_p^{(l-1)} = \sum_{n=0}^{P-1} \xi_n^{(l-1)} e^{-j\frac{2\pi}{P} n p}, \quad 0 \leq p \leq P-1. \quad (28)$$

Then, $E[|\Xi_p^{(l-1)}|^2]$ can be expressed as

$$\begin{aligned} E[|\Xi_p^{(l-1)}|^2] &= E \left[\sum_{n_1=0}^{P-1} \sum_{n_2=0}^{P-1} \xi_{n_1}^{(l-1)} (\xi_{n_2}^{(l-1)})^* e^{-j\frac{2\pi}{P} (n_1 - n_2) p} \right] \\ &= P E \left[|\xi_n^{(l-1)}|^2 \right]. \end{aligned} \quad (29)$$

Based on the previously stipulated assumption that the decision error always corrupts a symbol to one of the adjacent symbols, it becomes clear that the TD decision error signal only has four possible values, i.e., $\pm\alpha$ and $\pm j\alpha$, with α being the horizontal or vertical distance between adjacent symbols. This implies that $E[|\xi_n^{(l-1)}|^2] = P_s^{(l-1)} \alpha^2$. Therefore, (29) can be rewritten as

$$E[|\Xi_p^{(l-1)}|^2] = P P_s^{(l-1)} \alpha^2. \quad (30)$$

Note that the TD signal power is $\sigma_s^2 = \alpha^2/\beta$. From (25), (27), and (30), we have

$$\frac{|\Gamma^{(l-1)}|}{\sigma_S^2} < \frac{\sqrt{P P_s^{(l-1)}} \alpha \sigma_S}{\sigma_S^2} = \sqrt{P_s^{(l-1)}} \frac{\alpha}{\sigma_s} = \sqrt{\beta P_s^{(l-1)}}. \quad (31)$$

On the other hand, the SER at the detector's output should normally be less than 0.1 so that the DFE can reliably detect the received

signal. This level of the SER value can normally be achieved by the initial linear equalization. This means that $\sqrt{\beta P_s^{(l-1)}} \ll 1$. Thus, (31) indicates $|\Gamma^{(l-1)}| \ll \sigma_S^2$, and we have the following approximate relations:

$$\sigma_S^2 + \Gamma^{(l-1)} \approx \sigma_S^2 \quad (32)$$

$$\sigma_S^2 + 2\Re[\Gamma^{(l-1)}] \approx \sigma_S^2. \quad (33)$$

Estimation of Noise Power: For the given constellation mapping, there exists an SNR threshold above which the receiver becomes capable of meeting the target performance requirement. Therefore, we could use this predefined SNR value SNR_{pre} and approximate σ_W^2 by

$$\sigma_W^2 \approx \sigma_S^2 \cdot \text{SNR}_{\text{pre}}^{-1}. \quad (34)$$

C. Low-Complexity DFE Architecture

We are now ready to derive our simplified design. First, noting (26), we have $\sigma_{\Xi}^2 \ll \sigma_S^2$. Furthermore, upon setting $P_s^{(l-1)} = P_{s,\text{pre}}$, we arrive at

$$\frac{\sigma_S^2}{\sigma_S^2 + \sigma_{\Xi}^2} = \frac{1}{1 + \beta P_{s,\text{pre}}} \approx 1 \quad (35)$$

$$\frac{\sigma_{\Xi}^2}{\sigma_S^2 + \sigma_{\Xi}^2} \approx \frac{\sigma_{\Xi}^2}{\sigma_S^2} = \beta P_{s,\text{pre}} \quad (36)$$

where we have $\beta = 2, 2/5$ and $2/21$ for 4QAM, 16QAM, and 64QAM, respectively.

Inserting the results of (32)–(36) into (24), we have

$$\Phi = \sigma_S^2 \Phi^{(l-1)} \approx \frac{1}{P} \sum_{p=0}^{P-1} \frac{|H_p|^2}{\text{SNR}_{\text{pre}}^{-1} + \beta P_{s,\text{pre}} |H_p|^2}. \quad (37)$$

Similarly, (23) can be approximated as

$$\gamma = \gamma^{(l)} \approx \frac{\Phi}{1 + \Phi}. \quad (38)$$

Finally, the coefficients of the feedforward and feedback filters in (20) and (22) can be approximated as

$$C_p = C_p^{(l)} \approx \frac{(1 - \gamma) H_p^*}{\text{SNR}_{\text{pre}}^{-1} + \beta P_{s,\text{pre}} |H_p|^2} \quad (39)$$

$$B_p = B_p^{(l)} \approx -(C_p H_p - \gamma). \quad (40)$$

It is seen from (37)–(40) that, in this simplified FD-DFE, the parameters of the feedforward equalizer and feedback filter can be kept unchanged in each iteration based on the estimated channel frequency response. Therefore, we only have to compute these parameters once and do not have to update them at each iteration, as the IBDFFE does. This will significantly simplify the implementation of the equalizer, reducing its complexity.

Specifically, since the system structure of Fig. 1 is also adopted for the proposed FD-DFE, the computational complexity of the IDFT and DFT signal processing imposed on the proposed FD-DFE is the same as that of the IBDFFE. However, the parameter calculations of our architecture recorded for L iterations are beneficially simplified to be

$$12P + 1 \text{ multiplications, } 8P \text{ additions.} \quad (41)$$

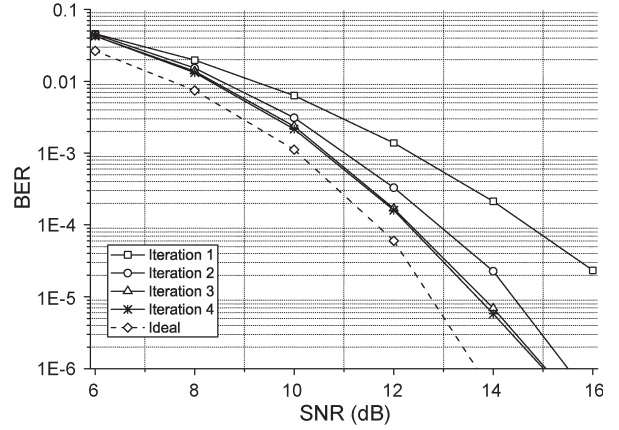


Fig. 2. BER performance of the proposed DFE for the SUI-4 channel. The preset parameters are $\text{SNR}_{\text{pre}} = 10$ dB and $P_{s,\text{pre}} = 0.1$.

Compared with the computational complexity of the IBDFFE given in (9), we can see that considerable computational savings are achieved, especially for a high number of iterations. We will demonstrate in the following simulation study that the performance of our simplified scheme is not sensitive to the choices of $P_{s,\text{pre}}$ and SNR_{pre} and that our low-complexity algorithm achieves the same BER performance as the IBDFFE.

IV. SIMULATION STUDY

The performance of the proposed low-complexity iterative FD-DFE was evaluated by simulations, using the IBDFFE as the benchmark. Uncoded 4QAM modulation was used with the symbol rate $f_s = 3$ MSymbols/s, and the size of the DFT was set to $P = 128$. Two typical multipath fading channels were chosen, i.e., the Stanford University Interim 4 (SUI-4) channel model [18] and the International Telecommunication Union (ITU) Vehicular A (ITU V-A) channel model [19]. Since the maximum delay spreads of these two channels were equal to the durations of 12 and eight symbols, respectively, $N = 16$ was used for the PN extension. The synchronization and the channel estimation were assumed to be ideal. The coefficients of the feedforward and feedback equalizers were computed based on (37)–(40), and we used $\text{SNR}_{\text{pre}} = 10$ dB and $P_{s,\text{pre}} = 0.1$. The results were obtained by averaging over 100 channel realizations in each case.

The BERs of the proposed iterative DFE recorded for iterations of 1–4 under these two multipath fading channels are shown in Figs. 2 and 3, respectively. The achievable performance under the error-free decision feedback is also provided for comparison (labeled as “ideal”). The result of the first iteration corresponds to the MMSE-based FD-LE (MMSE-FD-LE). From Figs. 2 and 3, we note that the second iteration yields a significant performance gain, compared with the MMSE-FD-LE. For example, under the SUI-4 channel, an SNR gain of about 2 dB can be achieved at the BER level of 2×10^{-5} , compared with the MMSE-FD-LE, whereas the gain is about 2.3 dB at the BER level of 3×10^{-4} for the ITU V-A channel. For both channels, three iterations were sufficient for the proposed DFE to converge since further iterations provided almost no gain, which is similar to the trends observed for the IBDFFE [14]. Compared with the results of ideal error-free feedback, the performance loss at iteration 3 is about 0.8 dB for the SUI-4 channel at $\text{BER} = 2 \times 10^{-5}$ and about 1.8 dB for the ITU V-A channel at $\text{BER} = 3 \times 10^{-4}$, respectively. Fig. 4 compares the BER of the proposed low-complexity DFE with that of the IBDFFE for the two channels. For simplicity, only the BER performance of the third iteration was recorded, as three iterations are sufficient for

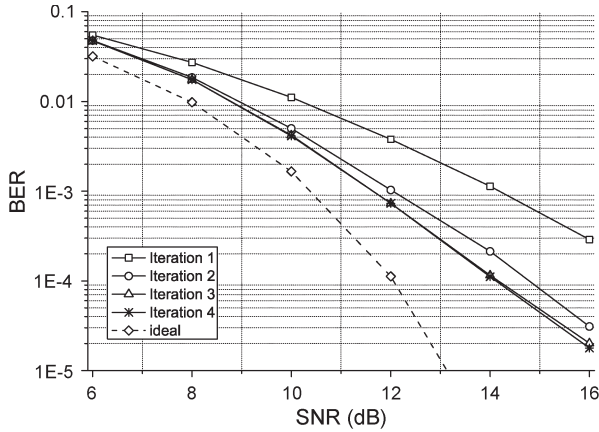


Fig. 3. BER performance of the proposed DFE for ITU V-A channel. The preset parameters are $\text{SNR}_{\text{pre}} = 10$ dB and $P_{s,\text{pre}} = 0.1$.

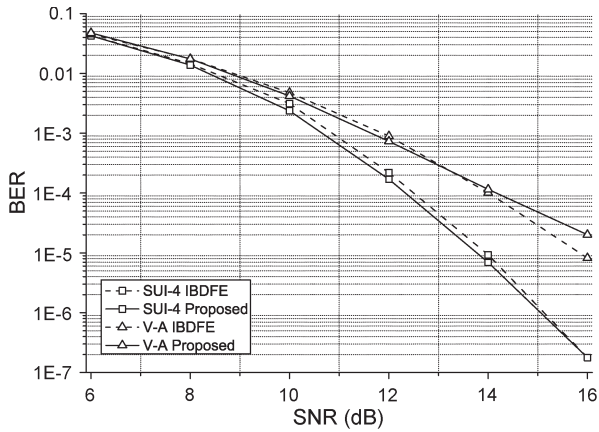


Fig. 4. BER performance comparison of the proposed low-complexity DFE and the IBDFE benchmark for both the SUI-4 and ITU V-A channels. The preset parameters for the low-complexity DFE are $\text{SNR}_{\text{pre}} = 10$ dB and $P_{s,\text{pre}} = 0.1$.

both equalizers. It can be seen in Fig. 4 that the proposed reduced-complexity DFE has similar performance to the IBDFE for both fading channels. More explicitly, the proposed simplified algorithm shows almost no performance degradation yet imposes a significantly lower computational complexity than the IBDFE benchmark.

The robustness of the proposed low-complexity DFE to the accuracy of $P_{s,\text{pre}}$ and SNR_{pre} used was demonstrated in Figs. 5 and 6. In Fig. 5, the BER performance is shown for $P_{s,\text{pre}} = 0.15, 0.1$, and 0.05 , respectively, while fixing $\text{SNR}_{\text{pre}} = 10$ dB. By contrast, given the fixed value of $P_{s,\text{pre}} = 0.1$, Fig. 6 shows the BER performance obtained for $\text{SNR}_{\text{pre}} = 8$ dB, 10 dB, and 12 dB, respectively. Again, only the BER curves corresponding to the third iteration were used. The results obtained clearly confirm that the proposed low-complexity FD-DFE is insensitive to the choices of $P_{s,\text{pre}}$ and SNR_{pre} values. These two values may be flexibly chosen for the given modulation scheme according to an expected minimum performance requirement. To further demonstrate the robustness of the proposed low-complexity FD-DFE to these two preset parameters, we plot the BER performance as the function of $P_{s,\text{pre}}$ and SNR_{pre} for both channels in Fig. 7, given the SNR value of 10 dB.

V. CONCLUSION

We have proposed a low-complexity iterative DFE for SC wireless systems that operates in the frequency domain based on the

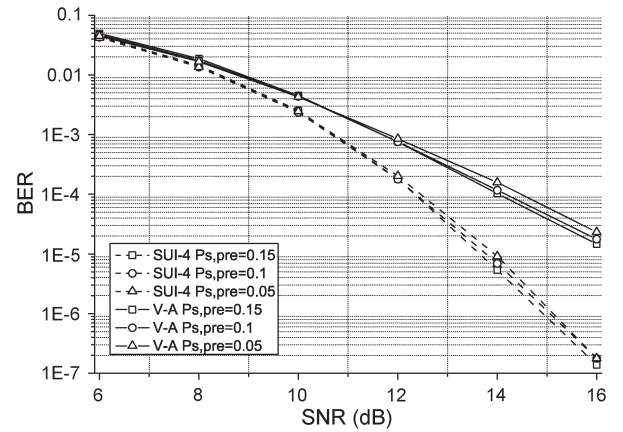


Fig. 5. BER performance of the proposed low-complexity DFE with different $P_{s,\text{pre}}$ values and given $\text{SNR}_{\text{pre}} = 10$ dB for both the SUI-4 and ITU V-A channels.

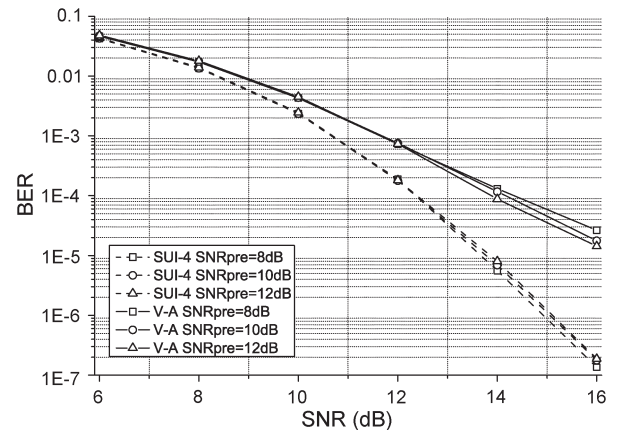


Fig. 6. BER performance of the proposed low-complexity DFE with different SNR_{pre} values and given $P_{s,\text{pre}} = 0.1$ for both the SUI-4 and ITU V-A channels.

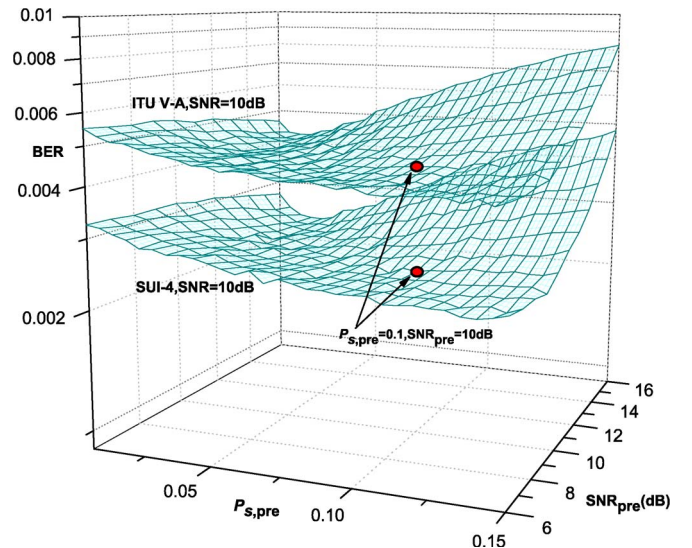


Fig. 7. BER performance of the proposed low-complexity DFE as a function of $P_{s,\text{pre}}$ and SNR_{pre} for both the SUI-4 and ITU V-A channels, given the SNR value of 10 dB.

MMSE criterion. The parameters of the feedforward and feedback equalizers in our simplified design only have to be computed once, rather than updating them in each iteration. This facilitates a simpler hardware implementation as a benefit of its reduced computational complexity, in comparison with the IBDFFE. Our simulation results have shown that the performance of this low-complexity FD-DFE is similar to that of the conventional IBDFFE benchmark under different multipath channels. The robustness of the proposed simplified design to the design parameters SNR_{pre} and $P_{s,\text{pre}}$ has also been confirmed.

REFERENCES

- [1] D. Falconer, S. L. Ariyavisitakul, A. Benyamin-Seeyar, and B. Eidson, "Frequency domain equalization for single carrier broadband wireless systems," *IEEE Commun. Mag.*, vol. 40, no. 4, pp. 58–66, Apr. 2002.
- [2] F. Pancaldi, G. M. Vitetta, R. Kalbasi, N. Al-Dhahir, M. Uysal, and H. Mheidat, "Single-carrier frequency domain equalization," *IEEE Signal Process. Mag.*, vol. 25, no. 5, pp. 37–56, Sep. 2008.
- [3] L. Hanzo, M. Münster, B. J. Choi, and T. Keller, *OFDM and MC-CDMA for Broadband Multi-User Communications, WLANs and Broadcasting*. Chichester, U.K.: Wiley, 2003.
- [4] *IEEE Standard for Wireless LAN Medium Access Control (MAC) and Physical Layer (PHY) Specifications*, IEEE Std. 802.11, Nov. 1997.
- [5] *Digital Video Broadcasting (DVB); Framing Structure, Channel Coding and Modulation for Digital Terrestrial Television*, ETSI EN 300 744, v1.5.1, Nov. 2004.
- [6] F. Khan, *LTE for 4G Mobile Broadband: Air Interface Technologies and Performance*. Cambridge, U.K.: Cambridge Univ. Press, 2009.
- [7] A. Czylik, "Comparison between adaptive OFDM and single carrier modulation with frequency domain equalization," in *Proc. VTC*, Phoenix, AZ, May 4–7, 1997, vol. 2, pp. 865–869.
- [8] *Draft IEEE Standard for Local and Metropolitan Area Networks—Part 16: Air Interface for Fixed Broadband Wireless Access Systems*, IEEE Std. 802.16-REVd/D5-2004, May 2004.
- [9] H. Sari, G. Karam, and I. Jeanclaude, "Transmission techniques for digital terrestrial TV broadcasting," *IEEE Commun. Mag.*, vol. 33, no. 2, pp. 100–109, Feb. 1995.
- [10] H. Witschnig, M. Kemptner, R. Weigel, and A. Springer, "Decision feedback equalization for single carrier system with frequency domain equalization—An overall system approach," in *Proc. 1st Int. Symp. Wireless Commun. Syst.*, Port Louis, Mauritius, Sep. 20–22, 2004, pp. 26–30.
- [11] Y. Zhu and K. B. Letaief, "Single carrier frequency domain equalization with noise prediction for broadband wireless systems," in *Proc. GLOBECOM*, Dallas, TX, Nov. 29–Dec. 3, 2004, vol. 5, pp. 3098–3102.
- [12] S. Ahmed, T. Ratnarajah, M. Sellahurai, and C. F. N. Cowan, "Reduced-complexity iterative equalization for severe time-dispersive MIMO channels," *IEEE Trans. Veh. Technol.*, vol. 57, no. 1, pp. 594–600, Jan. 2008.
- [13] M. Sabbaghian and D. D. Falcone, "An analytical approach for finite block length performance analysis of turbo frequency-domain equalization," *IEEE Trans. Veh. Technol.*, vol. 58, no. 3, pp. 1292–1301, Mar. 2009.
- [14] N. Benvenuto and S. Tomasin, "Iterative design and detection of a DFE in the frequency domain," *IEEE Trans. Commun.*, vol. 53, no. 11, pp. 1867–1875, Nov. 2005.
- [15] A. V. Oppenheim, R. W. Schaffer, and J. R. Buck, *Discrete-Time Signal Processing*. Upper Saddle River, NJ: Prentice-Hall, 1999.
- [16] D. R. Pauluzzi and N. C. Beaulieu, "A comparison of SNR estimation techniques for the AWGN channel," *IEEE Trans. Commun.*, vol. 48, no. 10, pp. 1681–1691, Oct. 2000.
- [17] F. Sainte-Agathe and H. Sari, "New results in iterative frequency-domain decision-feedback equalization," in *Proc. EUSIP*, Florence, Italy, Sep. 4–8, 2006, pp. 1–4.
- [18] *Channel Models for Fixed Wireless Applications*, IEEE Std. 802.16.3c-01/29r4, 2001.
- [19] *Guidelines for Evaluation of Radio Transmission Technologies for IMT-2000*, ITU-R Recommendation M.1225, 1997.

Performance of a Concurrent Link SDMA MAC Under Practical PHY Operating Conditions

Pengkai Zhao, Babak Daneshrad, Ajit Warrier,
Weijun Zhu, and Oscar Takeshita

Abstract—Space division multiple access (SDMA)-based medium access control (MAC) protocols have been proposed to enable concurrent communications and improve link throughput in multi-input–multi-output (MIMO) ad hoc networks. For the most part, the works appearing in the literature make idealized and simplifying assumptions about the underlying physical layer and some aspects of the link adaptation protocol. The result is that the performance predicted by such works may not necessarily be a good predictor of the actual performance in a fully deployed system. In this paper, we look to introduce elements into the SDMA-MAC concept that would allow us to better predict their performance under realistic operating conditions. Using a generic SDMA MAC, we look at how the network sum throughput changes with the introduction of the following: 1) use of the more practical MMSE algorithm, instead of the zero-forcing or singular-value-decomposition-based nulling algorithms used for receive beamforming; 2) impact of channel estimation errors; 3) introduction of link adaptation mechanism specifically designed for concurrent SDMA MACs; and 4) incorporation of TX beamforming along with RX beamforming. Following on the transmission window during which concurrent transmissions are allowed by the MAC, we qualify the impact of each of these four elements in isolation. At the conclusion, the performance of a system that incorporates elements 1–4 is presented and compared against the baseline system, showing an improvement of up to five times in the overall network sum throughput.

Index Terms—Concurrent communications, medium access control (MAC), multi-input–multi-output (MIMO), space division multiple access (SDMA).

I. INTRODUCTION

Networks of multi-input–multi-output (MIMO) enabled nodes can use advanced eigenbeamforming and beamnulling techniques to enable concurrent communications and increase overall network throughput. This technique is loosely referred to as space division multiple access (SDMA), and several medium access control (MAC) protocols have appeared in the literature that can deliver concurrent transmissions in an ad hoc network of multiantenna MIMO enabled nodes [1]–[5].

Although SDMA and concurrent links have been well studied in cellular networks (see [6] and the references therein), it is still a challenging problem in ad hoc networks. Initially, SDMA and concurrent links were utilized in ad hoc networks via a simple abstract model called degree of freedom (DOF) [7], [8]. This model uses the number of antennas to represent the number of concurrent links in the network. It assumes that the concurrent links are perfectly separated and do not interfere with one another. As such, the DOF model ignores all physical (PHY) layer impairments. At the same time, using TX/RX beamforming, the SPACEMAC, MIMAMAC, and NullHoc protocols [1]–[5] have been proposed to support concurrent links in

Manuscript received April 13, 2010; revised August 21, 2010 and November 1, 2010; accepted December 9, 2010. Date of publication December 30, 2010; date of current version March 21, 2011. The review of this paper was coordinated by Prof. H.-H. Chen.

P. Zhao and B. Daneshrad are with the Department of Electrical Engineering, University of California at Los Angeles, Los Angeles, CA 90095 USA.

A. Warrier, W. Zhu, and O. Takeshita are with Silvus Technologies, Inc., Los Angeles, CA 90024 USA.

Color versions of one or more of the figures in this paper are available online at <http://ieeexplore.ieee.org>.

Digital Object Identifier 10.1109/TVT.2010.2103096